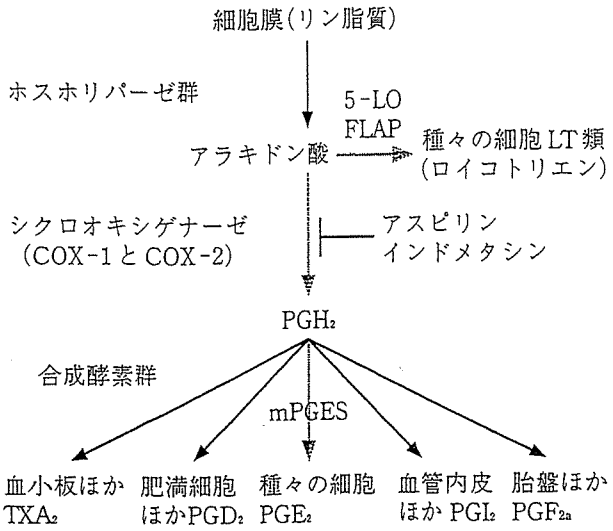

図5 プロスタグランジン産生系

3. 創薬の標的として注目されているプロスタグランジン合成酵素群の構造解析

シクロオキシゲナーゼ(COX)はプロスタグランジン(PG)を生合成する律速酵素として知られている(図5)2種類のアイソザイムが存在する．COX-1はconstitutive enzymeと呼ばれ，ほとんどの細胞で常時発現しており，生体の安定性を維持する役割を果たす．一方，COX-2はinducible enzymeとして，単球，線維芽細胞，滑膜細胞などの炎症にかかわる細胞で発現し，炎症性サイトカインなどによって誘導される．従来の非ステロイド系抗炎症剤は，COX-1とCOX-2の両方を阻害するために炎症巣のPGだけでなく，胃粘膜や腎でのPG(特にPGE_2)産生を抑制し胃や腎の副作用を合併する．そこで，炎症に深く関与していると考えられるCOX-2だけを選択的に阻害する薬剤の開発が進められてきた．このようにして開発されたCOX-2阻害薬は胃潰瘍を起こしにくい鎮痛剤として好んで投薬されていた．しかしながら，2004年末，米政府は，これらのCOX-2選択的阻害薬の3剤を心筋梗塞や脳梗塞の危険性を高める恐れがあるとして，心臓病患者への処方や多量の長期使用を避けるよう勧告した．COX-2の下流に位置するプロスタサイクリン合成酵素の作用も抑制するために，同酵素に由来する抗血栓性作用や血流増加作用が損なわれることが原因ではないかと考えられている[8]．図5に示したようにCOX-2の下流には多くの合成酵素があってそれぞれの作用を有する蛋白を合成している．個々の合成酵素を選択的に阻害する薬剤の開発が次世代の創薬の標的として注目される．PGE_2の産生にかかわるmPGESを阻害する薬物の開発は血管内血栓形成を伴わない理想的な抗炎症剤となる可能性がある．TXA_2産生を阻害する薬剤の開発は血管内血栓形成の予防，局所血流増加作用を通じて脳梗塞，心筋梗塞の予防薬や治療薬として期待できる．PGI_2は既に難病といわれた原発性肺高血圧症の治療に有効であることが知られている．PG関連薬剤の開発は構造に基づく創薬の最大の標的の一つになっており，ナノメディシンプロジェクトでも複数の関連酵素の構造解析に取り組んでいる．

4. ナノメディシンプロジェクトのそのほかの研究

本プロジェクトでは分子構造イメージングに関連して上記のほかに，細胞内イオン環境や，血管新生にかかわる蛋白など幾つかの蛋白構造についても研究を進めている(国立循環器病センター研究所)．国立精神神経センターではin-silicoスクリーニング法によるParkinson病の治療薬探索に蛋白構造情報を応用する研究を進めている．国立医薬品食品衛生研究所では原子間力顕微鏡を用いて蛋白表面の詳細な構造を解析することなどを通じて，医用材料作成に向けた応用研究に取り組んでいる．

一方，分子機能イメージングの領域では，国立循環器病センターの望月らが増殖因子(EGF)刺激に伴うRas分子の活性化をFRET法で可視化できることをNature誌に報告した[9]．ナノメディシンプロジェクト開始後も血管内皮の走化運動にかかわるRap1蛋白の可視化に関する研究などにFRET法による分子イメージングを展開している．国立精神神経センターの研究グループでは分子機能イメージング技術を応用してシナプス機能，プリオン蛋白質の機能の評価に

取り組み Proc Natl Acad Sci などの雑誌に研究成果を報告している[10].

おわりに

本ナノメディシンプロジェクトでは循環器治療の中核施設である国立循環器病センター内に構造生物学ラボを立ち上げ，分子特異的な治療薬の開発を目指している．ナノ DDS 技術や分子機能イメージング技術に関する研究を併せて推進することで，特異的分子治療薬の分子輸送技術開発と他の分子との相互作用の可視化技術を推進することが可能となる．これにより，分子診断・分子治療・分子評価を包含するテーラーメード医療の基盤形成に貢献したい．

謝辞 本原稿の執筆内容は本研究グループの成果を元にしております．国立循環器病センター研究所若林繁夫分子生理部長およびユーセフ・ベン・アマー同研究員，増田道隆循環器形態部室長，柴田洋之心臓生理部同室員，五十嵐智子同研究員，松原孝宜同研究員，大阪大学月原富武教授，理化学研究所宮野雅司主任研究員に感謝いたします．また，本原稿編集と英文作成に協力していただいた東本弘子女史，松尾千重女史に感謝します．

文献

1) Patick AK, et al: Activities of the human immunodeficiency virus type 1(HIV-1) protease inhibitor nelfinavir mesylate in combination with reverse transcriptase and protease inhibitors against acute HIV-1 infection in vitro. Antimicrob Agents Chemother 41: 2159-2164, 1997.
2) Drucker BJ, et al: Effects of a selective inhibitor of the Abl tyrosine kinase on the growth of Bcr-Abl positive cells. Nat Med 2: 561-566, 1996.
3) Takeda S, et al: Structure of the core domain of human cardiac troponin in the Ca^{2+} saturated form. Nature 424: 35-41, 2003.
4) 前田雄一郎ほか：トロポニンの結晶構造とカルシウム調節のメカニズム．蛋白質 核酸 酵素 48: 500-512, 2003.
5) 大槻磐男：筋収縮カルシウム受容調節の分子機構と遺伝性機能障害．日薬理誌 118: 147-158, 2001.
6) Lee JA, et al: Effects of pimobendan, a novel inotropic agent on intracellular calcium and tension in isolated ferret ventricular muscle. Clin Sci 76: 609-618, 1989.
7) Nieminen MS, et al: Executive summary of the guidelines on the diagnosis and treatment of acute heart failure: The task force on acute heart failure of the European society of cardiology. Eur Heart J 26: 384-416, 2005.
8) Mukherjee D, et al: Risk of cardiovascular events associated with selective cox-2 inhibitors. JAMA 286: 954-959, 2001.
9) Mochizuki N, et al: Spatio-temporal images of growth-factor-induced activation of Ras and Rap1. Nature 411: 1065-1068, 2001.
10) Itami C, et al: Brain-derived neurotrophic factor-dependent unmasking of silent synapses in developing mouse barrel cortex. Proc Natl Acad Sci USA 100: 13069-13074, 2003.

Altered Emotional Behaviors in Mammalian Bombesin Receptor Knockout Mice: Implication for the Molecular Pathogenesis of Stress-Induced Psychiatric Disorders in Humans

Keiji Wada, Kazuyuki Yamada, Yuko Santo-Yamada, Hiroshi Maeno, Etsuko Wada, and Masayuki Sekiguchi

1. Introduction

Neuropeptides are thought to play important roles in the pathogenesis of various psychiatric disorders, including posttraumatic stress disorder (PTSD) (Merali et al. 2002). To elucidate the pathophysiological role of neuropeptides for the disorders in vivo, we have employed behavioral analyses of gene-manipulated mice lacking their receptors. Among various neuropeptides, we have focused on bombesin, because its receptors are highly expressed in the hippocampus and the amygdala. Both regions are known to mediate memory and emotional behaviors.

Bombesin (BN) is a tetradecapeptide originally purified from the skin of the European frog *Bombina bombina* (Anastasi et al. 1971). Two BN-like peptides, gastrin-releasing peptide (GRP) and neuromedin B (NMB), have been identified in mammalian tissues (McDonald et al. 1979; Minamino et al. 1983). These peptides exert their effects by binding to G-protein coupled receptors on the cell surface; these are the GRP-preferring receptor (GRP-R) and the NMB-preferring receptor (NMB-R). In addition, a third subtype of mammalian bombesin receptor (BRS-3) has been cloned; however, high affinity natural ligand(s) specific to BRS-3 have not yet been identified (Battey and Wada 1991; Fathi et al. 1993). BN-like peptides and their receptors are widely distributed in the mammalian central nervous system and modulate many aspects of behavior such as spontaneous activity and feeding behavior, as well as learning and memory (Flood and Morley 1988; Flynn 1991; Kirkham et al. 1993; Santo-Yamada et al. 2001). We previously produced three strains of BN-like peptide receptor knockout mice using a gene-targeting method (Ohki-

National Institute of Neuroscience, National Center of Neurology and Psychiatry, Ogawahigashi, Kodaira, Tokyo 187-8502, Japan
Brain Science Institute, RIKEN, Wako, Saitama 351-0198, Japan

Hamazaki et al. 1997, 1999; Wada et al. 1997). The resulting mice, deficient in GRP-R, NMB-R, and BRS-3, were used in studies designed to clarify and distinguish the functional properties of BN-like peptides in the brain. As a result, we found that the NMB/NMB-R system may work as a risk factor for stress vulnerability and that the GRP/GRP-R system may play some role in learning and memory.

2. NMB and NMB-R

We investigated the effect of restraint stress on the behavior of NMB-R-deficient mice. We first examined the maternal behavior of the mice before and after the stress for 30 min (Yamada et al. 2002a). Near the end of the stress, three pups were laid individually in corners of each home cage. Immediately following the stress treatment, each experimental virgin female mouse was introduced into the vacant corner of the home cage. The essential maternal indices (licking, pup retrieval, grouping, nesting, and crouching) were measured in the initial and final 5-min observation periods during a 35-min test session. As shown in Fig. 1, the overall ma-

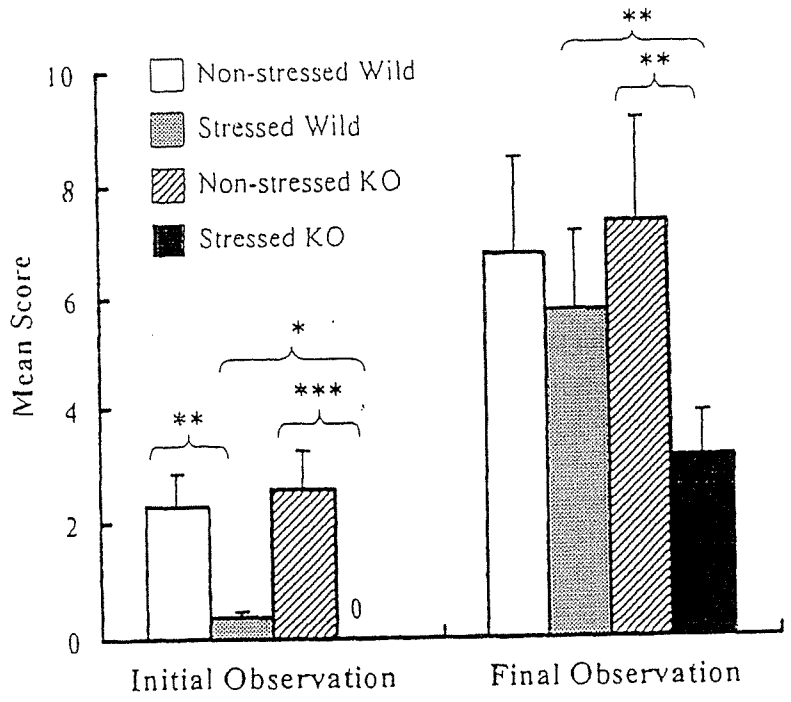

Fig. 1. Overall maternal behavioral performance of neuromedin B-preferring receptor (NMB-R)-deficient mice (*KO*) and wild-type mice with/without 30-min restraint-induced stress. The overall scores represent the sum of the scores of the individual components: pup retrieval, grouping, crouching, and nesting. Data given as mean + quartile deviation. *Asterisks* represent statistical significance between the indicated groups: *** $P < 0.0001$; ** $P < 0.005$; * $P < 0.03$

ternal indices at the final observation were significantly lower in stressed NMB-R-deficient mice compared with those of stressed wild-type control mice. At the initial observation, we did not find significant difference of the indices between the two genotypes with stress. The maternal behaviors of wild-type and NMB-R-deficient mice are both suppressed in the initial observations. Furthermore, nonstressed mice show similar indices between the two genotypes. These results suggest that restraint-induced stress can impair maternal behavior in mice, and NMB-R-deficient mice may suffer more severely from the stress than wild-type mice.

Similar vulnerability of NMB-R-deficient mice to the restraint stress was observed in the inhibitory avoidance learning (Yamada et al. 2003). Using a one-trial passive avoidance test, stressed NMB-R-deficient mice exhibited a marked reduction in memory performance (Fig. 2). In the test trial, we did not observe any difference in the mean step-through latency between nonstressed NMB-R-deficient and wild-type mice; however, stressed NMB-R-deficient mice showed significantly shorter latency than stressed wild-type mice and nonstressed NMB-R-deficient mice (Fig. 2). Although NMB-R-deficient mice exhibited elevated spontaneous activity in a novel environment (open field) compared with nonstressed mutant mice after 30 min of stress, a similar difference was also observed between stressed/nonstressed wild-type mice. An elevated plus maze test did not show any effect of the stress stimulus on anxiety in either wild-type or NMB-R-deficient mice. Furthermore, pain response of wild-type and NMB-R-deficient mice induced by electric

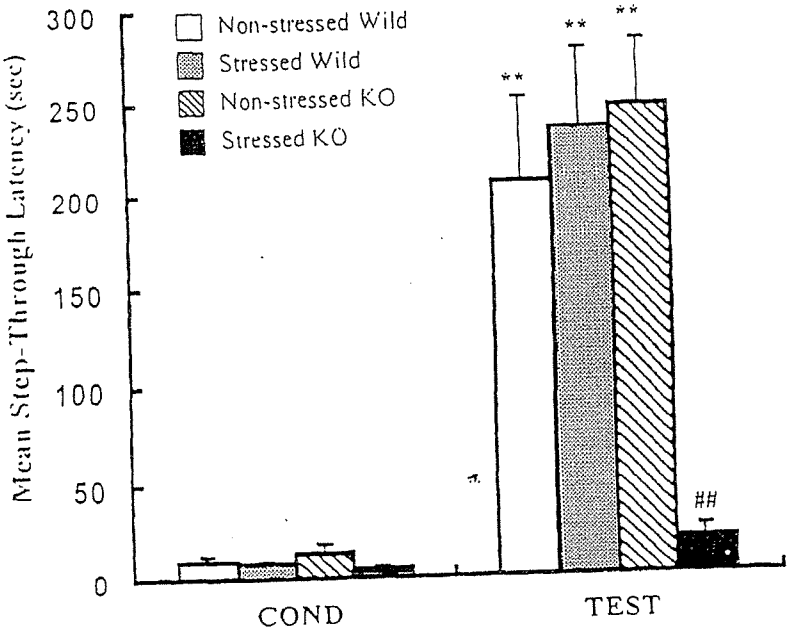

Fig. 2. One-trial passive avoidance test. Data given as mean + SEM. *Asterisks* indicate statistical significance between the acquisition trial and the test trial ($P < 0.01$); *hashes* indicate statistical significance between stressed NMB-R-deficient mice and stressed wild-type mice or nonstressed NMB-R-deficient mice in the test trial ($P < 0.01$). *COND*, acquisition trial; *TEST*, test trial

footshock was not affected under either stressed or nonstressed conditions. These results indicate that impaired memory performance in stressed NMB-R-deficient mice is not a consequence of changes in spontaneous activity, anxiety, or pain response, and suggest that the NMB/NMB-R pathway plays a role in regulating the stress response via the neural system that controls learning and memory.

We then evaluated the risk assessment behavior of the mice using two representative behavioral paradigms, the light-dark (L-D) box test and the elevated plus maze test (Yamada et al. 2002b). In the L-D box test, there were no significant differences between mutant mice and their wild-type littermates with respect to the conventional parameters such as dark-light (D-L) latency and the duration of staying in the light compartment. However, in the analysis of risk assessment behavior (stretched attend posture), NMB-R-deficient mice exhibited a significant decrease in risk assessment behavior relative to the wild-type cohort (data not shown). Similar to the results of the L-D box test, the analyses of risk assessment behavior from the elevated plus maze test revealed that NMB-R-deficient mice displayed a relative decrease in the frequency of this posture (data not shown). Although risk assessment behavior has yet to gain broad consent as a behavioral index of anxiety, there are reports that this behavior may reflect some emotional state of animals (Yamada et al. 2002b).

Our results suggest that the NMB/NMB-R pathway modulates some forms of emotion (perhaps including anxiety) and constitutes one of the risk factors of stress vulnerability. NMB-R-deficient mice should provide useful information for molecular pathogenesis of stress-induced disorders. Because the NMB/NMB-R system possibly interacts with 5-hydroxytryptamine (5-HT) neurons (Yamada et al. 2002c), further studies should reveal the neural circuits responsible for stress-induced mental disorders including PTSD.

3. GRP and GRP-R

We investigated the role of the GRP/GRP-R system in memory and learning. We first examined the effect of GRP peptide in wild-type mice with drug-induced amnesia. GRP was administered following training in a one-trial passive avoidance test. When scopolamine was used to induce amnesia prior to training, GRP (32 nmol/kg, ip) improved memory performance when the dosage of scopolamine was relatively low (1 mg/kg, ip). We then examined the role of GRP for the acquisition of inhibitory avoidance learning in mice using GRP-R antagonists. An administration of [Leu^{13}-(CH_2NH)-Leu^{14}]BN (antagonizes GRP-R > NMB-R) impaired the performance of inhibitory avoidance learning in all doses (16, 32, 64 nmol/kg). These results suggest that the GRP/GRP-R system plays an important role in memory and learning. Recently, GRP was shown to be important for inhibiting memory specifically related to learned fear (Shumyatsky et al. 2002). We generated specific antibody against the receptor, and found that the antibody is an excellent tool for investigating the expression of GRP-R in the brain (Kamichi et al. 2005). Double-

labeling immunohistochemistry demonstrated that subpopulations of GRP-R are present in GABAergic neurons in the amygdala. Consequently, GRP-R immunoreactivity was observed in the GABAergic neurons of the limbic region. These anatomical results support the idea that the GRP/GRP-R system mediates memory performance by modulating neurotransmitter release in the local GABAergic network.

4. Conclusion

Our results indicate that the NMB-R-deficient mouse is an important tool for investigating the molecular mechanism of stress-induced disorders and developing therapeutic drugs for the disorders. Besides the NMB/NMB-R system, the GRP/GRP-R system is likely to be involved in fear memory. Thus, it is likely that the mammalian bombesin system plays a role in regulating stress response through the neural system that controls learning and memory. Further investigation of the involvement of the mammalian bombesin system in PTSD should provide useful information for the treatment of the disease.

References

Anastasi A, Erspamer V, Bucchi M (1971) Isolation and structure of bombesin and alytensin, two analogous active peptides from the skin of the European amphibians Bombina and Alytes. Experientia 27:166–167

Battey J, Wada E (1991) Two distinct receptor subtypes for mammalian bombesin-like peptides. Trends Neurosci 14:524–528

Fathi Z, Corjay MH, Shapira H, Wada E, Benya R, Jensen R, Viallet J, Sausville EA, Battey JF (1993) BRS-3: a novel bombesin receptor subtype selectively expressed in testis and lung carcinoma cells. J Biol Chem 268:5979–5984

Flood JF, Morley JE (1988) Effects of bombesin and gastrin-releasing peptide on memory processing. Brain Res 460:314–322

Flynn FW (1991) Effects of fourth ventricle bombesin injection on meal-related parameters and grooming behavior. Peptide 12:761–765

Kamichi S, Wada E, Aoki S, Sekiguchi M, Kimura I, Wada K (2005) Immunohistochemical localization of gastrin-releasing peptide receptor in the mouse brain. Brain Res 1032:162–170

Kirkham TC, Perez S, Gibbs J (1993) Prefeeding potentiates anorectic actions of neuromedin B and gastrin-releasing peptide. Physiol Behav 54:467–470

McDonald TJ, Jornvall H, Nilsson G, Vagne M, Ghatei M, Bloom SR, Mutt V (1979) Characterization of a gastrin releasing peptide from porcine non-antral gastric tissue. Biochem Biophys Res Commun 90:227–233

Merali Z, Kent P, Anisman H (2002) Role of bombesin-related peptides in the mediation or integration of the stress response. Cell Mol Life Sci 59:272–287

Minamino N, Kangawa K, Matsuo H (1983) Neuromedin B: a novel bombesin-like peptide identified in porcine spinal cord. Biochem Biophys Res Commun 114:541–548

Ohki-Hamazaki H, Watase K, Yamamoto K, Ogura H, Yamano M, Yamada K, Maeno H, Imaki J, Kikuyama S, Wada E, Wada K (1997) Mice lacking bombesin receptor subtype-3 develop metabolic defects and obesity. Nature 390:165–169

Ohki-Hamazaki H, Sakai Y, Kamata K, Ogura H, Okuyama S, Watase K, Yamada K, Wada K (1999) Functional properties of two bombesin-like peptide receptors revealed by the analysis of mice lacking neuromedin B receptor. J Neurosci 19:948–954

Santo-Yamada Y, Yamada K, Wada K (2001) Post-training administration of gastrin-releasing peptide (GRP) improves memory loss in scopolamine- and hypoxia-induced amnesic mice. Physiol Behav 74:139–143

Shumyatsky GP, Tsvetkov E, Malleret G, Vronskaya S, Hatton M, Hampton L, Battey JF, Dulac C, Kandel ER, Bolshakov VY (2002) Identification of a signaling network in lateral nucleus of amygdala important for inhibiting memory specifically related to learned fear. Cell 111:905–918

Wada E, Watase K, Yamada K, Ogura H, Yamano M, Inomata Y, Eguchi J, Yamamoto K, Maeno H, Mikoshiba K, Ohki-Hamazaki H, Wada K (1997) Generation and characterization of mice lacking gastrin-releasing peptide receptor. Biochem Biophys Res Commun 239:28–33

Yamada K, Santo-Yamada Y, Wada K (2002a) Restraint stress impaired maternal behavior in female mice lacking the neuromedin B receptor (NMB-R) gene. Neurosci Lett 330:163–166

Yamada K, Santo-Yamada Y, Wada E, Wada K (2002b) Role of bombesin (BN)-like peptides/receptors in emotional behaviour by comparison of three strains of BN-like peptide receptor knockout mice. Mol Psychiat 7:113–117

Yamada K, Wada E, Yamano M, Sun YJ, Ohara-Imaizumi M, Nagamatsu S, Wada K (2002c) Decreased marble burying behavior in female mice lacking neuromedin-B receptor (NMB-R) implies the involvement of NMB/NMB-R in 5-HT neuron function. Brain Res 942:71–78

Yamada K, Santo-Yamada Y, Wada K (2003) Stress-induced impairment of inhibitory avoidance learning in female neuromedin B receptor-deficient mice. Physiol Behav 78:303–309

European Journal of Neuroscience, Vol. 25, pp. 406–416, 2007 doi:10.1111/j.1460-9568.2007.05282.x

Truncated TrkB-T1 regulates the morphology of neocortical layer I astrocytes in adult rat brain slices

Koji Ohira,[1,2,3] Nobuo Funatsu,[1] Koichi J. Homma,[4] Yoshinori Sahara,[1] Motoharu Hayashi,[5] Takeshi Kaneko,[2,3] and Shun Nakamura[1,3]

[1]Department of Biochemistry and Cellular Biology, National Institute of Neuroscience, National Center of Neurology and Psychiatry, 4-1-1 Ogawahigashi, Kodaira, Tokyo 187–8502, Japan
[2]Department of Morphological Brain Science, Graduate School of Medicine, Kyoto University, Kyoto 606–8501, Japan
[3]Core Research for Evolutional Science and Technology (CREST), Japan Science and Technology Agency, Saitama 332–0012, Japan
[4]Department of Molecular Pathology, Faculty of Pharmaceutical Sciences, Teikyo University, Kanagawa 199–0195, Japan
[5]Department of Cellular and Molecular Biology, Primate Research Institute, Kyoto University, Aichi 484–8506, Japan

Keywords: BDNF, electroporation, neurotrophin, RNA interference

Abstract

By altering their morphology, astrocytes, including those involved in the maintenance and plasticity of neurons and in clearance of transmitter, play important roles in synaptic transmission; however, the mechanism that regulates the morphological plasticity of astrocytes remains unclear. Recently, we reported that T1, a subtype of TrkB (a family of BDNF-specific receptors), altered astrocytic morphology through the control of Rho GTPases in primary astrocyte cultures. In this study, we extended this observation to investigate acute neocortical slices from adult rats. T1 siRNA-expression vectors were electroporated into astrocytes in neocortical layer I of living rats. In both normal slices and control vector-electroporated slices, BDNF induced the elongation of the astrocytic processes and increased the branching of processes in slices after 1 h incubation. In contrast, in T1 siRNA-electroporated slices, no such significant morphological changes were observed in the astrocytes. In addition, the number of synaptophysin$^+$ sites in contact with GFAP$^+$ processes increased in a BDNF–T1-dependent manner without the increase in the total synaptophysin$^+$ sites. Therefore, the present study provides evidence of the regulation of layer I astrocytic morphology by the BDNF–T1 signal in adult rat neocortical slices.

Introduction

Neurotrophins and their specific tropomyosin-related kinase (Trk) receptors are known to be involved in the regulation of cell morphology during development (Bibel & Barde, 2000). Neurotrophins (NTs) belong to the nerve growth factor (NGF)-related gene family: NGF, brain-derived neurotrophic factor (BDNF), NT-3, and NT4/5. The Trk receptor family consists of three members: TrkA for NGF, TrkB for BDNF and NT-4/5, and TrkC for NT-3 (Barbacid, 1994). The *trkB* gene encodes at least three receptor subtypes (Klein *et al.*, 1990; Middlemas *et al.*, 1991). One such subtype is the full-length form (TK+) that includes tyrosine kinase in the cytosolic domain. The other two subtypes, T1 and T2, lack tyrosine kinases. T1 is expressed in both neurons and glial cells (Armanini *et al.*, 1995; Ohira *et al.*, 2005a, 2005b) whereas T2 is expressed primarily in neurons (Armanini *et al.*, 1995).

Recent studies have shed light on interactions between neurons and glial cells (Fellin & Carmignoto, 2004). In particular, it has been demonstrated that calcium entry into astrocytes modulates synaptic transmission (Bezzi *et al.*, 2004; Fiacco & McCarthy, 2004). In addition, astrocytic endfeet enwrap synapses (Ventura & Harris, 1999), i.e. those synapses referred to as tripartite synapses (Araque *et al.*, 2001). Interestingly, astrocytic processes surrounding active synapses are able to rapidly alter their morphology in acute slices from the brainstem (Hirrlinger *et al.*, 2004), hypothalamus (Langle *et al.*, 2003) and hippocampus (Benediktsson *et al.*, 2005) of infant- to pubertal-stage rodents. In contrast, alterations of fine neuronal structures such as dendrites and spines in the neocortex of adult mice hardly occur under normal conditions (Grutzendler *et al.*, 2002). Such results have suggested that the morphological alteration of astrocytes might be essential for the maintenance and plasticity of synaptic transmission, as well as for transmitter clearance. Therefore, it would be of great interest to clarify the mechanism(s) responsible for controlling astrocytic morphology.

Recently, we reported that T1 regulates astrocytic morphology via Rho GTPases in primary astrocyte cultures (Ohira *et al.*, 2005a). T1 also controls calcium entry into astrocytes (Rose *et al.*, 2003). In addition, BDNF release is highly regulated by neuronal activity (Hartmann *et al.*, 2001; Kohara *et al.*, 2001). Thus, these findings led us to postulate that BDNF release due to neuronal activity might induce morphological changes in astrocytes in the CNS.

For the initial evaluation of this hypothesis, we investigated the role played by endogenous T1 in the regulation of astrocytic morphology in acute slices of the adult rat neocortex. Using T1 small interfering RNA (siRNA)-expressing vectors that were electroporated into neocortical layer I of adult rats, we demonstrated that T1 regulated astrocytic

Correspondence: Dr Shun Nakamura, [1]Department of Biochemistry and Cellular Biology, as above.
E-mail: nakamura@ncnp.go.jp

Received 13 March 2006, revised 5 November 2006, accepted 7 November 2006

morphology in a BDNF-dependent manner. Therefore, considering that astrocytes modulate synaptic transmission (Bezzi *et al.*, 2004; Fiacco & McCarthy, 2004), these results indicate that the morphological changes regulated by the BDNF–T1 signal in astrocytes might play important roles in adult synaptic plasticity in the neocortex.

Materials and methods

T1 siRNA vector

The T1 siRNA vector was produced using the BLOCK-iT U6 Entry Vector kit (Invitrogen, Carlsbad, CA, USA). The pENTR/U6 vector integrates the human U6 promoter which drives RNA polymerase III. Generally, transcription by RNA polymerase III produces a higher amount of RNA than that by RNA polymerase II. Moreover, the U6 promoter belongs to a type III polymerase promoter, which is suitable for expressing a short-length RNA such as short hairpin RNA and micro RNA, for use in RNA interference because there is no internal promoter in it.

Briefly, 5′ oligo CAGCGTCATAAGATCCCCCTGGATGAGAATCCAGGGGGATCTTATGA and 3′ oligo AAAATCATAAGATCCCCCTGGATTCTCATCCAGGGGGATCTTATGAC were incubated at 95 °C for 4 min. The mixture was cooled to room temperature for 10 min to generate the double-strand oligo. The double-strand oligo was cloned into the pENTR/U6 vector. For the control oligos, 5′ oligo CAGCGAAGATCCCCCTGGATGGGAACGCCCATCCAGGGGGATCTT and 3′ oligo AAAAAAGATCCCCCTGGATGGGCGTTCCCATCCAGGGGGATCTTC were used.

Western blot analysis

C6 cells (Dainippon Pharmaceutical, Osaka, Japan) were maintained in Ham's F-10 medium (Gibco, Rockville, MD, USA) supplemented with 15% horse serum (Gibco) and 2.5% fetal bovine serum (Gibco) in a humidified atmosphere containing 5% CO_2 at 37 °C. The vectors (2 μg per 6-cm dish) were transfected into C6 cells (50% confluent) with FuGENE6 (Roche, Basel, Switzerland; Wiesenhofer *et al.*, 1999). The transfection efficiency of the green fluorescent protein (GFP) expression vector was ~ 60%. After 24 h, the cells were lysed in lysis buffer (Tris-HCl, pH 7.5, 50 mM; NaCl, 150 mM; $MgCl_2$, 5 mM; Triton X-100, 0.5%; PMSF, 1 mM; leupeptin, 10 μg/mL; and aprotinin, 20 μg/mL). After the lysed cells were centrifuged at 10 000 *g* at 4 °C for 20 min, the supernatants were mixed with 4 × sodium dodecyl sulphate (SDS) sample buffer and boiled for 3 min. Samples (5 μg/lane for actin and tubulin, 100 μg/lane for T1) were subjected to SDS–polyacrylamide gel electrophoresis (7% gel for T1, 12% gel for actin and tubulin), and the proteins were blotted onto polyvinylidene difluoride membranes (Millipore, Billerica, MA, USA). The membranes were blocked in 5% skimmed milk in phosphate-buffered saline (PBS; in mM: NaCl, 137; Na_2HPO_4, 8.1; KCl, 2.7; and KH_2PO_4, 1.5). After incubation of the blots with antibodies (anti-T1, diluted at 1 : 200; Santa Cruz Biotech., Santa Cruz, CA, USA; antiactin, diluted at 1 : 200; and antitubulin, diluted at 1 : 200; both Sigma, St Louis, MO, USA) at room temperature for 1 h, they were incubated with secondary antibodies conjugated with horseradish peroxidase and the proteins were visualized by the enhanced chemiluminescence system (Amersham Pharmacia Biotech, Tokyo, Japan). The specificity of anti-T1 antibody for use with Western blot analysis and immunohistochemistry has already been assessed in our previous studies (Ohira *et al.*, 1999; Ohira & Hayashi, 2003). For the quantitative analysis of protein bands we measured the band areas using ImageJ software.

Electroporation

The methods were approved by the National Institute of Neuroscience Committee for the Ethical use of Experimental Animals, based on the guiding principles of the Council for International Organizations of Medical Sciences (1984). Every effort was made to minimize the number of animals used. Adult male Sprague–Dawley (S-D) rats (4–6 weeks, n = 10) were deeply anaesthetized with sodium pentobarbital (50 mg/kg). A rectangular hole in the right hemisphere of the skull (3 mm wide and 5 mm long) was created. After an anode tungsten needle was stereotaxically and diagonally inserted under the neocortex (2 mm posterior and 3.5 mm lateral to the bregma, at an angle of 20° to the brain surface), a mixture of 20 μL (GFP : siRNA, 1 : 5) of GFP plasmid vector solution (pCA-GFP; 1 μg/μL in 0.01% Fast Green in Tyrode's solution) and T1 siRNA (1 μg/μL) or the control vectors (1 μg/μL) was injected between the arachnoid and the dura using a pipette (P-20; Gilson, Middleton, WI, USA) connected to a silicon tube and a 27-gauge injection needle (Terumo, Tokyo, Japan). The rectangular platinum plate cathode (1 mm wide and 1.5 mm long) was placed on the dura, and a series of five square pulses (50 ms, 15 V, 950-ms intervals) were immediately sent using Electro Square Porator model T820 and Optimizor 500 (BTX, Harvard Apparatus, Holliston, MA, USA). At 3 days after electroporation, the rats were killed and the brains were removed in order to prepare acute slices.

Morphological assay

Rats were anaesthetised with pentobarbital sodium (25 mg/kg i.p.). After decapitation, the brains were removed from normal (4–6 weeks S-D rat, n = 10) and electroporated rats (4–6 weeks S-D rat, n = 10) and yellow fluorescent protein (YFP) transgenic mice [4–6 weeks, n = 3; B6.Cg-Tg (Thy1-YFP) 16Jrs/J, The Jackson Laboratory, Bar Harbor, ME, USA], and 500-μm slices were created. The slices were kept for 30 min at 4 °C in DMEM (Invitrogen, Carlsbad, CA, USA) containing N2 supplement (Invitrogen). For the administration of reagents, the slices were stimulated for 60 min at 37 °C and 5% CO_2 with 20 ng/mL BDNF (PeproTech, Rocky Hill, NJ, USA) or 100 ng/mL NGF (PeproTech). The dishes were agitated gently during incubation. Then, the slices were fixed at 4 °C for 1 h in 4% PFA in PBS. For cryoprotection, they were sequentially immersed in 5, 10, 20 and 30% sucrose. Thereafter, the slices were further sliced into 10-μm-thick sections and were incubated with the primary antibodies at 4 °C for 48 h. For the double staining analysis, we used the following primary antibodies: the rabbit polyclonal antibodies were antiglial fibrillary acidic protein (GFAP; diluted at 1 : 50; Sigma) and anti-T1 (diluted at 1 : 1600; Santa Cruz Biotech.); and the mouse monoclonal antibodies were antiglutamic acid decarboxylase 65/67 (diluted at 1 : 10 000; Affinity Research Products, Exeter, UK), anti-GFAP (diluted at 1 : 1000; Chemicon, Temecula, CA, USA), and antisynaptophysin (diluted at 1 : 1000; Chemicon). For the T1 staining procedure, in order to retrieve antigenicity the samples were preincubated in 6 M guanidine chloride in 50 mM Tris-HCl, pH 10.2, for 15 min at room temperature (Ohira *et al.*, 2003, 2004, 2005a, 2005b). For the morphological analyses of the astrocytes, the parameters were defined as follows: a thick process that extended radially from a soma was defined as a primary process, and a fine process that extended from a primary process was designated a branch. For the analysis of synaptophysin-positive ($^+$) sites, the number of sites per 14 500 μm^2 was counted. For the analysis of the interaction among synaptophysin$^+$ sites and GFAP$^+$ processes, the number of synaptophysin$^+$ sites that were piled on (white in Fig. 6A and B) or contacted with GFAP$^+$ processes (blue in Fig. 6A and B) was counted

in an area of 14 500 μm^2. The samples in a 0.5-μm-thick plane were analysed using a confocal microscope (TCS SP2; Leica. Wetzlar, Germany). In this assay, we chose the layer I areas to be analysed at random.

For the quantitative analysis of *in vivo* fluorescent intensity of T1, the images of astrocytes were taken under the same condition. Fluorescent intensity was measured with ImageJ software.

Terminal deoxynucleotidyl transferase-mediated digoxigenin nucleotide nick-end labelling (TUNEL) staining

Apoptotic cells were identified by using modified ApopTag apoptosis detection systems (Serologicals, Norcross, GA, USA). For the analyses of injured cortices, young adult male S-D rats (4–6 weeks, $n = 3$) were deeply anaesthetized with sodium pentobarbital (50 mg/kg). Rectangular holes were bored into the skull (3 mm wide and 5 mm long) over the right hemisphere. The motor cortex was injured by the application of a surgical knife attached to the tip of the vertical bar of the stereotaxic instrument; this procedure was performed according to the stereotaxic brain atlas (Paxinos & Watson, 1986). The stereotaxic coordinates used for cutting were as follows: anteroposterior, −1 to −1.5 mm from bregma; lateral, 4 mm from the midline; and depth, 1 mm below the brain surface. At 2 days after the operation, the brains were fixed in 4% PFA. The brain sections (10 μm) from the injured and electroporated rats were incubated with terminal deoxynucleotidyl transferase for 1 h at 37 °C. Thereafter, the sections were stained with antidigoxigenin (Roche Applied Science, Basel, Switzerland) and with secondary antibody conjugated with Cy3 (Chemicon). Nuclei were stained with Hoechst 33258 (Sigma).

Data collection

In the following two analyses (the astrocytic morphology and the relationship between $GFAP^+$ processes and $synaptophysin^+$ sites), we obtained the data from 10 normal rats, five control vector-electroporated rats and five T1 siRNA vector-electroporated rats. In addition, one control and one siRNA vector-electroporated rat was subjected to each analysis.

In order to analyse astrocytic morphology, we collected data from 57 cells in normal slices not treated with BDNF, 63 cells in normal slices treated with BDNF, 62 cells in normal slices not treated with NGF, 60 cells in normal slices treated with NGF, 71 cells in control vector-electroporated slices not treated with BDNF, 75 cells in control vector-electroporated slices treated with BDNF, 71 cells in siRNA vector-electroporated slices not treated with BDNF and 66 cells in siRNA vector-electroporated slices treated with BDNF. For the analysis of the relationship between $GFAP^+$ processes and $synaptophysin^+$ sites, the data was obtained from the following: 44 normal sections not treated with BDNF, 47 normal sections treated with BDNF, 43 normal sections not treated with NGF, 45 sections treated with NGF, 47 control vector-electroporated sections not treated with BDNF, 46 control vector-electroporated sections treated with BDNF, 49 siRNA vector-electroporated sections not treated with BDNF and 48 siRNA vector-electroporated sections treated with BDNF.

Results

BDNF-dependent morphological change in astrocytes in neocortical layer I of acute slices prepared from adult rats

Astrocytes in the CNS are generally divided into two groups, fibrous and protoplasmic astrocytes. Fibrous astrocytes are characterized by (i) long processes with slight branching, (ii) GFAP-rich contents and (iii) distribution in the white matter and in neocortical layer I. Protoplasmic astrocytes have the following typical features: (i) well-branching short processes, (ii) low GFAP content and (iii) distribution in the grey matter (Peters *et al.*, 1976; Raff *et al.*, 1983; Miller & Raff, 1984). In the present study an immunofluorescent approach was used to observe layer I fibrous astrocytes, but the protoplasmic astrocytes in layers II–VI were not observed. As GFAP was observed in large amounts in the layer I fibrous astrocytes, a double-immunofluorescence study of GFAP and T1 enabled the visualization of layer I fibrous astrocytes (Fig. 1A). Also, the layer I fibrous astrocytes do not overlap their neighbours' space (Fig. 2). Similarly, the protoplasmic astrocytes in hippocampal CA1 stratum radiatum have separate domains (Bushong *et al.*, 2002). Therefore, we were able to observe individual astrocytes without any intermingling. Moreover, in our preliminary study we visualized the morphology of astrocytes in neocortical layer I of acute brain slices prepared from developing mice (postnatal days 14–20) using a combination of intracellular recording, biocytin injection and coimmunofluorescent staining with GFAP. These findings were in contrast to those obtained with protoplasmic astrocytes, in which GFAP only enables the visualization of ~15% of the total cell volume in the hippocampal CA1 (Bushong *et al.*, 2002). The layer I astrocytes exhibited a mean resting membrane potential of −77.3 ± 7.0 mV (total $n = 8$ cells), and did not produce action potentials. The morphology revealed by biocytin injection into glial cells that had been electrophysiologically identified was consistent with that of neocortical layer I astrocytes in adult mammals (Colombo *et al.*, 2000). Although this intracellular staining method could reveal the morphology of astrocytes clearly in the developing cortex by 3 weeks postnatal, it was impracticable to make whole-cell patch-clamp recordings of astrocytes in adult slices of mice and rats. Our aim of this study was to determine whether T1 was involved in the regulation of morphological changes in astrocytes in the adult cortex. In this study, therefore, whole-cell patch-clamp recording was abandoned in favour of investigating the morphological changes in astrocytes in the adult cortex. In our rat preparation, a double-immunofluorescence study of GFAP and T1 expression revealed that the cell shape of neocortical layer I astrocytes was quite similar to that observed in the mouse preparation. The length of layer I astrocytes in our study (mean ± SD, 24.5 ± 9.2 μm; total, 194 processes from 57 astrocytes) was similar to the data reported by Colombo *et al.*, 2000). Thus, we concluded that the cell shape observed in the double-immunofluorescence study with GFAP and T1 probably reflects the actual cell bodies and processes of the astrocytes in layer I. We therefore focused on layer I fibrous astrocytes.

As shown in Fig. 1, we observed rapid morphological changes among layer I astrocytes with BDNF treatment for 1 h. BDNF treatment induced process elongation and branching, but it did not lead to an increase in the number of primary processes from each soma. In contrast, NGF treatment had no effect on astrocytic morphological changes. Together with the finding that the layer I astrocytes express mainly T1 *in vivo* (Ohira *et al.*, 2005a), this finding regarding morphological changes among astrocytes is suggestive of an induction by the T1 signalling cascade in the astrocytes themselves.

Effect of T1 siRNA on astrocytic morphology

Next, in order to examine the contribution of T1 to BDNF-dependent morphological changes in astrocytes, we constructed T1 siRNA-expression vectors. Then, using rat glioma C6 cells that intrinsically express T1, we confirmed the RNA interference effect of this vector (Fig. 3). At 24 h after transfection, the expression level of T1 had not changed in the control vector-transfected cells (Fig. 3B). On the other

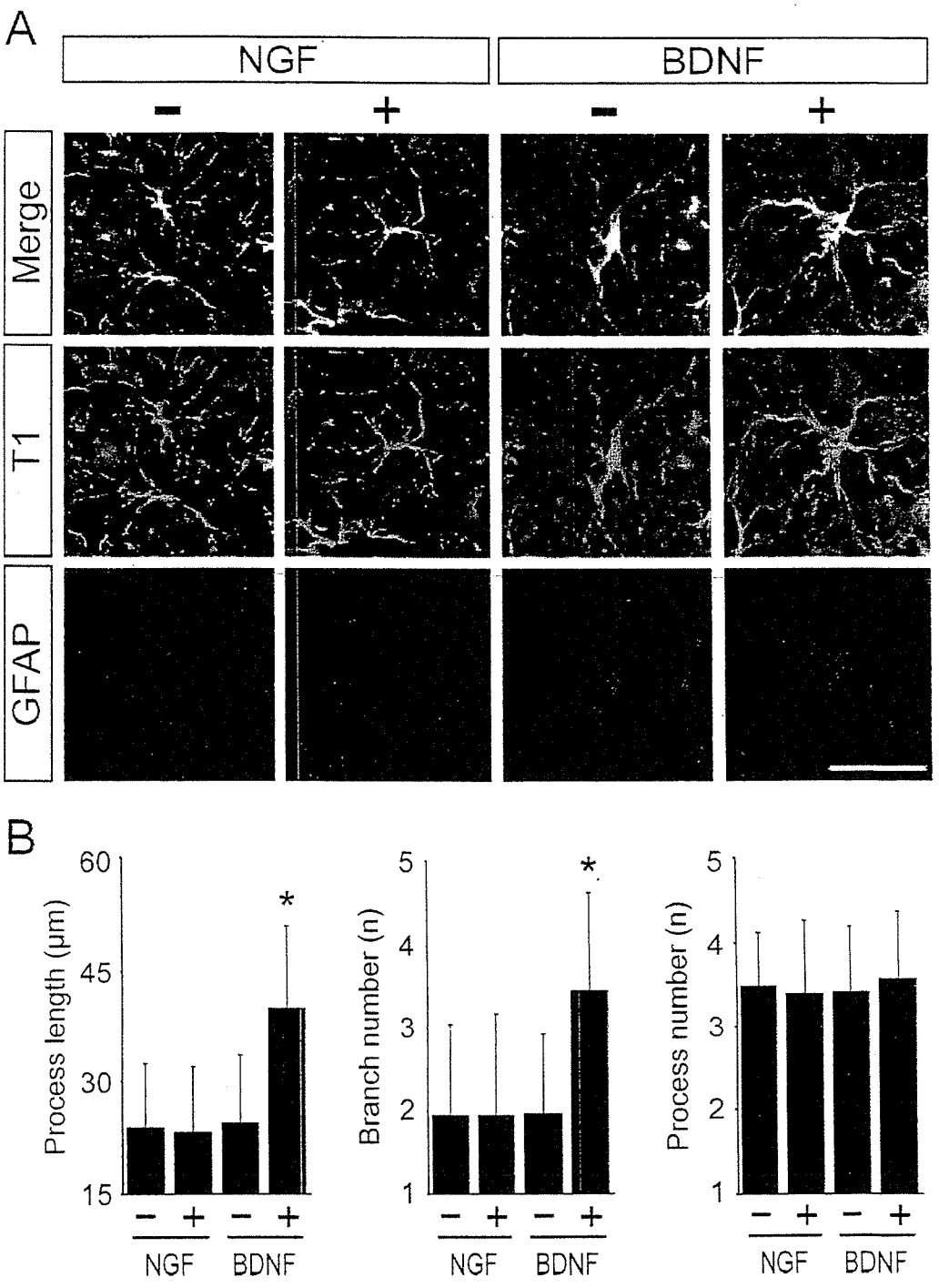

FIG. 1. Morphological changes in astrocytes. (A) Astrocytes in layer I of the motor cortex were stained by anti-T1 (blue) and anti-GFAP (red). (B) Quantitative analyses of process length (left panel), number of branches (middle panel) and number of processes (right panel). Values are given as means ± SD and are the results of four independent experiments. $*P < 0.05$ (one-way ANOVA and Scheffé's *post hoc* test) compared to the astrocytes in slices not treated with BDNF; -, no stimulation; −, stimulation with NGF or BDNF. Scale bar, 30 μm.

hand, in the T1 siRNA-transfected cells, T1 expression was decreased to 1/4 of the control level (Fig. 3B). Thus, we concluded that the T1 siRNA-expression vectors were effective at suppressing the expression of T1 proteins.

In order to deliver the T1 siRNA-expression vectors into the layer I astrocytes, we performed an electroporation of T1 siRNA-expression vectors into the neocortex of living rats. At 3 days after electroporation, the neocortical slices were subjected to a series of morphological analyses. The vectors were focally electroporated into layer I cells, such that we did not observe GFP expression in neurons and glial cells of layers II–VI. As this *in vivo* electroporation damaged brain tissue under the cathode plate, for this analysis we chose regions in which there were neither apoptotic nor necrotic cells in the electroporated tissues (Fig. 4). As a positive control for the TUNEL method we used brain tissues damaged with a surgical knife. In the control sections, apoptotic cells were observed (Fig. 4A–C), while there were no apoptotic cells in the neighbouring sections subjected to the morphological analysis of astrocytes (Fig. 4G–N). At the same

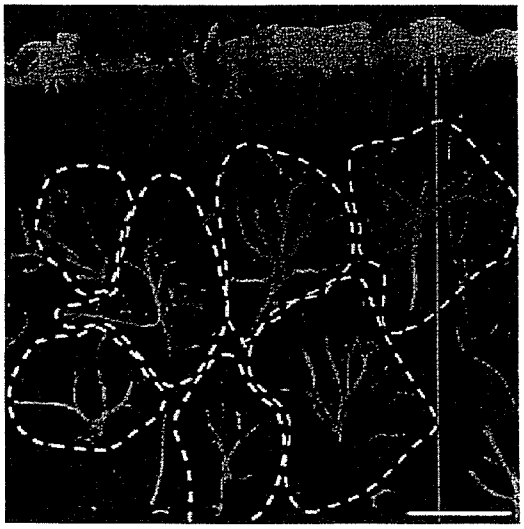

FIG. 2. Individual domains of layer I fibrous astrocytes. Astrocytes were visualized with anti-GFAP (green). The white dotted lines indicate the domain of each layer I fibrous astrocyte. Note that layer I fibrous astrocytes have separate domains, suggesting that we can observe the fine structures of astrocytes, such as processes and branching, without the problems of intermingling. Scale bar, 25 μm.

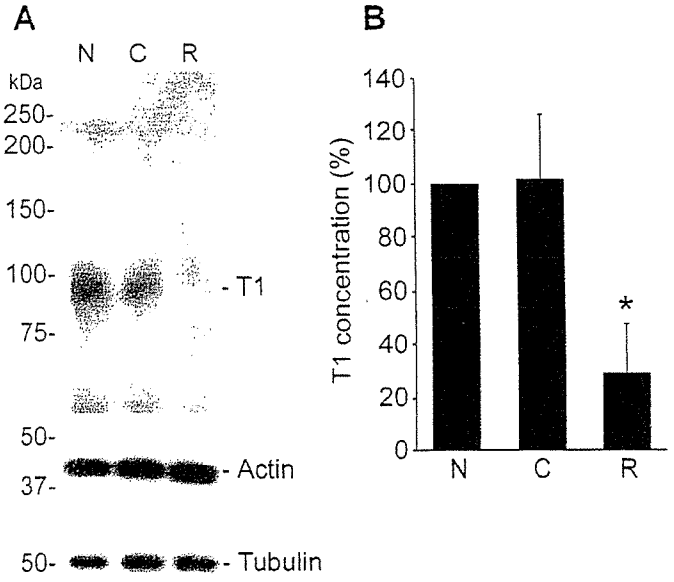

FIG. 3. Effect of T1 siRNA on T1 expression in C6 cells. (A) Either control vectors or T1 siRNA-expression vectors were transfected into C6 cells that intrinsically express T1. The expression of T1 was examined by Western blot analysis with anti-T1. The molecular weight of T1 was 95 kDa. The positions of the molecular weight markers are shown on the left. (B) Quantitative analysis of T1 bands in A. The expression level of T1 in the no transfection sample was taken as 100%. *$P < 0.05$ (one-way ANOVA) compared to the level of the no transfection sample. Values are given as means ± SD and were obtained from three independent experiments, and a representative image is shown. N, no transfection; C, control vector; R, siRNA vector.

time we assumed that the T1 siRNA-expression vector had been transferred into the astrocytes; this assumption was based on the expression of GFP, the expression vector of which was cotransferred with the siRNA vectors. In addition, it was observed that the GFP-expressing astrocytes did show a reduction in the T1 expression level (panel T1 in Fig. 5A).

To determine the *in vivo* efficiency of T1 siRNA, the quantitative analysis of *in vivo* T1 expression in the control- or siRNA-vector electroporated astrocytes was performed by measuring the fluorescent intensity of T1. The fluorescent intensity of T1 in the siRNA vector-electroporated astrocytes was significantly decreased compared with that in the control vector-electroporated astrocytes (Fig. 5C). Therefore, based on T1 expression, the siRNA vector was effective.

In the slices prepared from control vector-electroporated rats, BDNF induced a significant increment in the length and number of branches of the processes, while no change in primary process number was observed (Fig. 5). These amounts of change were identical to those observed in the nonelectroporated slices (Figs 1 and 5). When not treated with BDNF, slices prepared from the T1 siRNA vector-electroporated rats showed no difference from those with control vectors. Also, the astrocytes containing T1 siRNA-expression vectors appeared to have fewer branches and shorter processes under the no-BDNF treatment condition, though this difference was not significant (Fig. 5B). This result might be caused by an increase in cytosolic Rho GTPases due to the reduced expression of T1, which might bind and retain Rho GDI1 in the cell membrane. When treated with BDNF and inhibited T1 expression, astrocytes exhibited slight, albeit not significant, elongation and branching of the processes (Fig. 5B). These slight increases in process length and branching might be due to the low level of T1.

Relationship of GFAP$^+$ processes and synaptophysin$^+$ sites

Morphological changes in astrocytes have effects on the clearance of neurotransmitters and the regulation of synaptic transmission (Theodosis & Poulain, 1993; Iino *et al.*, 2001; Oliet *et al.*, 2001; Theodosis *et al.*, 2004). Moreover, in the cerebellum, Bergmann glial cells receive glutamate via ectopic release, and functional AMPA receptors are densely distributed in the Bergmann glial membrane that faces the synaptic structures (Matsui *et al.*, 2005), suggesting that astrocytic processes in close proximity to synapses may be capable of locally regulating synaptic functions. Thus, in this study we also addressed the question of whether or not the BDNF–T1 signalling leads to an increase in the number of synapses that are in contact with GFAP$^+$ processes. In this analysis, there is the possibility that synaptophysin$^+$ sites might represent cut axonal fibres. We assessed this problem using YFP-transgenic mice. In these mouse brains, YFP proteins were strongly expressed in the cell body, axons and dendrites of the layer V pyramidal neurons (Feng *et al.*, 2000). If cut axonal fibre terminals (YFP$^+$) were also synaptophysin$^+$, we would have detected the synaptophysin and YFP double-positive sites. However, we hardly found any such double-positive sites. Therefore, we considered synaptophysin$^+$ sites to be actual mature synapses (Okabe *et al.*, 2001). As shown in Fig. 6A and C, the number of synaptophysin$^+$ sites in contact with GFAP$^+$ processes increased in a BDNF-dependent manner, presumably because of the BDNF-induced extension of the astrocytic processes and astrocytic branching. On the other hand, neither BDNF nor NGF treatment was found to influence the overall density of synaptophysin$^+$ sites (Fig. 6D).

Next, we examined the effect of T1 siRNA on the interaction between GFAP$^+$ processes and synaptophysin$^+$ sites. In the control vector-electroporated slices, the number of synaptophysin$^+$ sites that were in contact with GFAP$^+$ processes increased more than two-fold, a result which was compatible with the amounts in the nonelectroporated slices (Fig. 6C). In contrast, no morphological changes among the astrocytes were observed in the T1 siRNA-expression vector electroporated slices. Moreover, the reduction in the number of synaptophysin$^+$ sites in contact with GFAP$^+$ processes appeared to

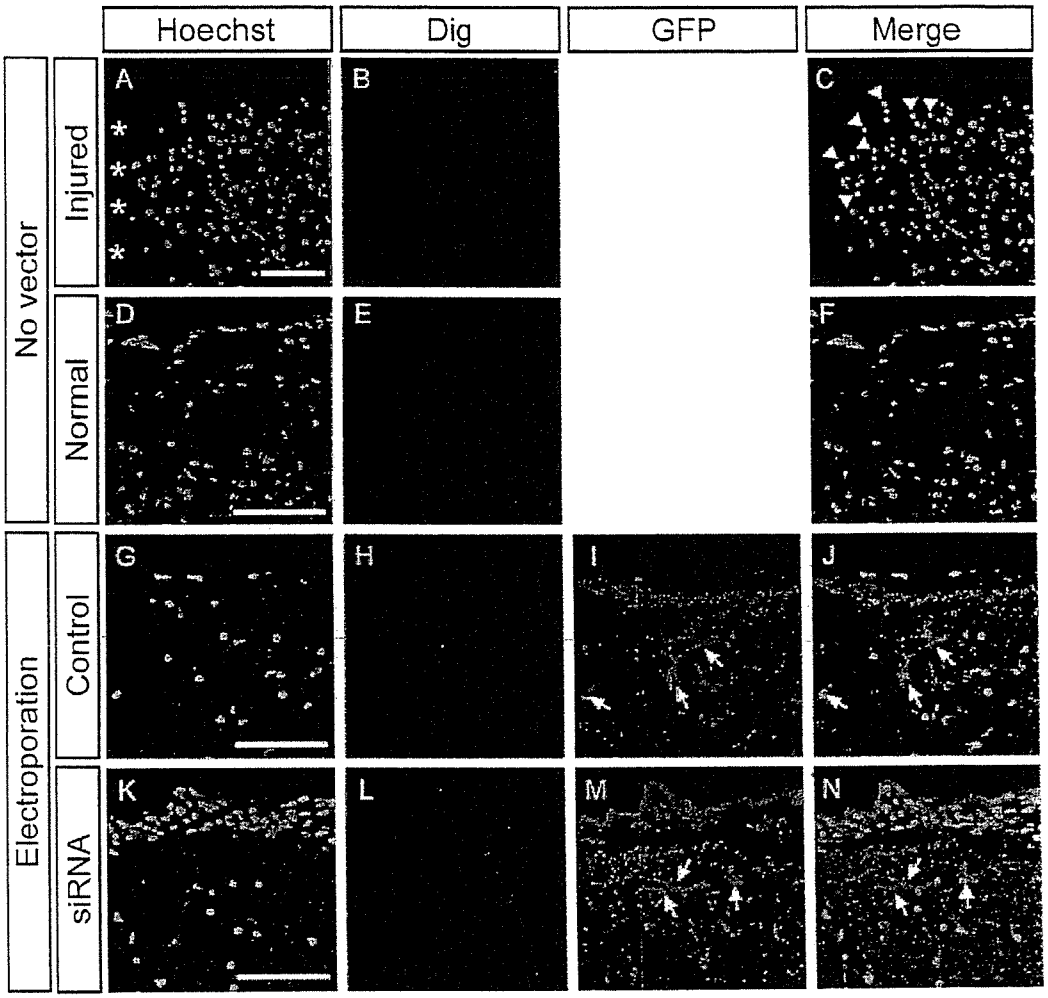

FIG. 4. Apoptotic cells in (A–C) injured, (D–F) unelectroporated, (G–J) control vector-electroporated, and (K–N) T1 siRNA vector-electroporated slices of the motor cortex. Apoptotic cells were detected by the TUNEL method with anti-Dig (B, E, H and L; red) and these cells are indicated by arrowheads. Electroporated cells expressed GFP (I and M; green cells indicated by arrows). Nuclei were stained with Hoechst 33258 (A, D, G, and K; blue). Note that the apoptotic cells, indicated by the arrowheads in C, were distributed around the injured region (asterisks in A), but were hardly detected in (E) the normal slices and in (H and L) the electroporated slices, thus suggesting that in these regions electroporation successfully delivered the plasmid vectors into neocortical layer I without inducing cell death. Scale bars, 100 μm.

reflect a decrease in $GFAP^+$ process length and in the branching induced by T1 siRNA, although this result was not significant (Fig. 6C).

Discussion

In this study, we demonstrated that BDNF regulated astrocytic morphology in adult neocortical slices via a truncated TrkB receptor, T1. Our data also revealed that the number of $synaptophysin^+$ sites in contact with $GFAP^+$ processes increased in a BDNF–T1-dependent manner without a change in the number of total $synaptophysin^+$ sites. Therefore, these results show that the neocortical layer I astrocytes exhibit high morphological plasticity in the adult rat brain.

Knock-down of T1 expression by siRNA and electroporation

In the present study, we performed *in vivo* knock-down of T1 by using T1 siRNA. The *trkB* gene contains at least three subtypes that have in common an extracellular domain, a transmembrane domain and the first 12 intracellular amino acid sequences. We designed the 19-mer oligonucleotide from adenosine at 1852 in the T1 sequence (GenBank accession number M55292). Interestingly, the control sequence started four nucleotides upstream of the T1 siRNA sequence. This control vector had virtually no RNAi effect on T1 expression (Fig. 3) or morphological changes in astrocytes (Figs 5 and 6), which was similar to the data from the normal rats (Figs 1 and 6). Although the cause was unknown, there was no great difference between the percentages of GC content in the two sequences. Thus, the secondary and/or tertiary structure of the resulting RNA might be the reason.

In this study, we performed electroporation to transfect the T1 siRNA-expression vectors into astrocytes. However, the electroporation and the cutting of slices kill the cells or weaken them. To choose the healthy areas in the slices, we checked the adjacent sections by the TUNEL method, which detects apoptotic cells. Also, we found gliosis as well as apoptosis at the margins of the areas damaged by electroporation. However, there was no gliosis in other areas (data not shown), because the electroporation of weak electric potential used in this study (five pulses of 50 ms, 15 V at 950-ms intervals) would cause limited focal damage, as reported in the previous studies (Kondoh *et al.*, 2000; Kachi *et al.*, 2005). Moreover, in the control vector-electroporated slices, the morphology of astrocytes (length,

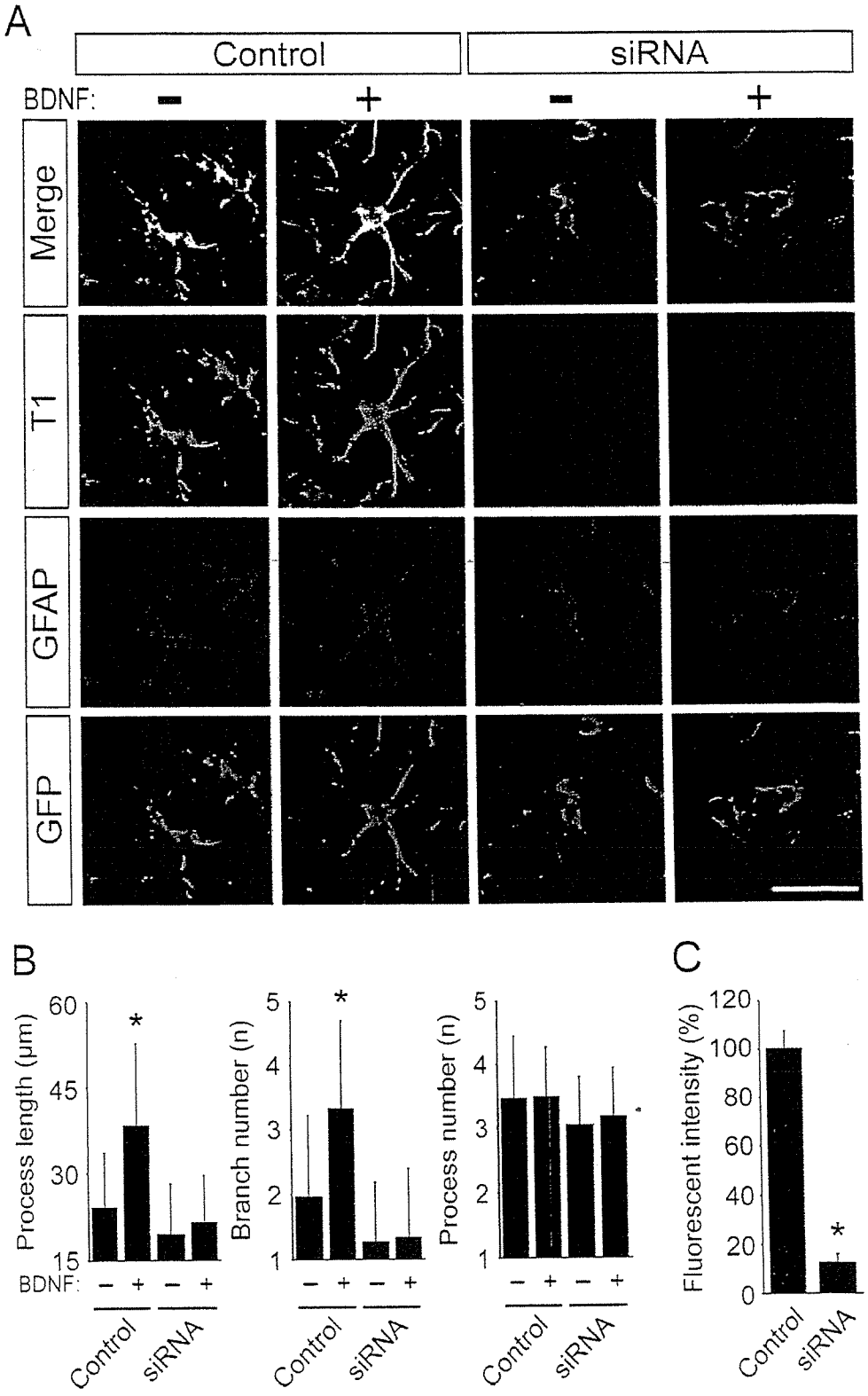

FIG. 5. Morphological changes in astrocytes transfected with T1 siRNA-expression vector. (A) Control or T1 siRNA-expression vector-electroporated astrocytes were visualized with anti-T1 (blue), anti-GFAP (red) and electroporated GFP (green). Slices were incubated for 60 min with BDNF (20 ng/mL) or vehicle (DMEM). Note that few T1-immunoreactive structures were observed in the T1 siRNA-expression vector-electroporated cells. (B) Quantitative analyses of process length (left panel), number of branches (middle panel) and number of processes (right panel). Values are given as means ± SD and are the results of four independent experiments. *$P < 0.05$ (two-way ANOVA) compared to astrocytes in the control slices not treated with BDNF. There was a significant difference in the BDNF treatment, but not a difference between the control- and the siRNA-expression vectors. (C) Quantitative analysis of T1 fluorescence intensity. Fluorescence intensity was measured with ImageJ. The expression level of T1 in the no transfection sample was taken as 100%. Values are given as means ± SD and are the results of four independent experiments. *$P < 0.05$, Student's *t*-test, between the T1 fluorescence intensity levels of the control and siRNA-expression vector transfected astrocytes. Control, electroporation of control vector; siRNA, electroporation of T1 siRNA-expression vector; –, no stimulation; +, stimulation with BDNF. Scale bar, 20 μm.

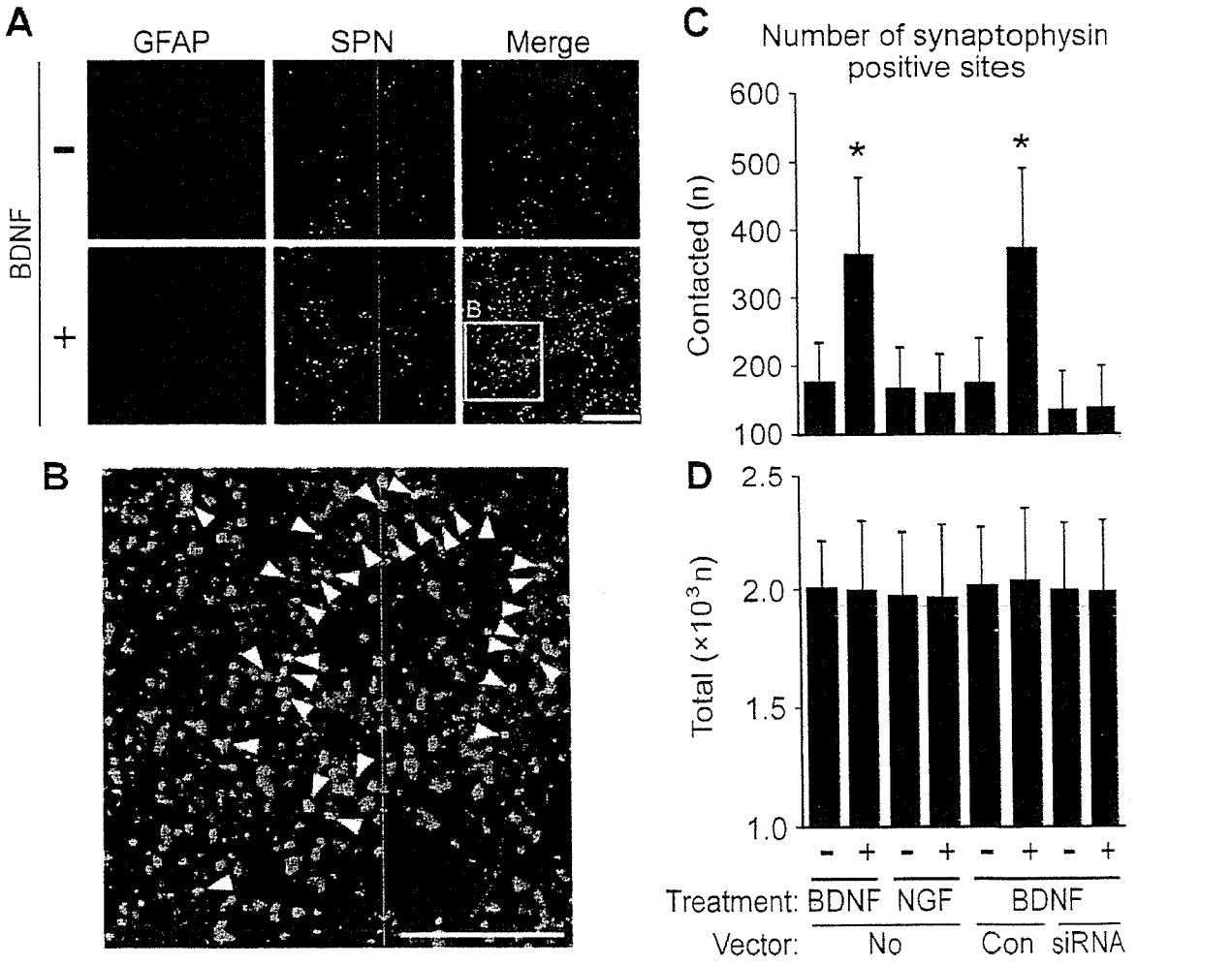

FIG. 6. Interaction between GFAP$^+$ processes and synaptophysin$^+$ sites. (A) Images of GFAP$^+$ processes (red) and synaptophysin (SPN)$^+$ sites (blue) in layer 1 of the motor cortex of normal acute slices. Slices were incubated for 60 min with BDNF (20 ng/mL) or vehicle (DMEM). (B) A high-powered image of the boxed-in area in A. Arrowheads indicate SPN$^+$ sites (white) in contact with GFAP$^+$ processes. (C and D) Quantitative analysis of (C) SPN$^+$ sites (white) in contact with GFAP$^+$ processes and (D) total SPN$^+$ sites. The normal slices, the control vector-electroporated slices and the RNAi vector-electroporated slices were treated with the indicated reagents: NGF (100 ng/mL), BDNF (20 ng/mL) and vehicle (DMEM). Values are given as means ± SD and are the results of four independent experiments. *P < 0.05 (one-way ANOVA and Scheffé's *post hoc* test) compared to the levels observed in astrocytes in normal slices not treated with BDNF; -, no stimulation; +, stimulation with NGF or BDNF. Scale bars, 20 μm.

branching and number of processes) was similar to that from the nontreated slices. Therefore, the morphology of astrocytes in the analysed areas was not affected by electroporation.

Subcellular localization of T1 and GFAP

The subcellular localization of T1 was very similar to that of GFAP (Figs 1 and 5). The single staining for T1 shows a uniform distribution of T1 in cell bodies and processes (Ohira *et al.*, 2005b). On the other hand, GFAP was also uniformly localized in the astrocytic cell bodies and processes (Fig. 2), suggesting that each specific antibody used here is not cross-reactive. Thus, these results indicate that proteins of both T1 and GFAP were distributed close to each other in astrocytes.

The colocalization of T1 and GFAP may indicate that T1 interacts with GFAP. In a previous study, we reported that T1 binds directly Rho GDI1, which is a negative regulator of a small G-protein family, Rho (Ohira *et al.*, 2005a). Additionally, T1 downregulates the activity of ROCK, a downstream effector kinase of RhoA, in a BDNF-dependent manner (Ohira *et al.*, 2006). Moreover, ROCK phosphorylates GFAP, which causes depolymerization of GFAP (Kosako *et al.*, 1997). Thus, T1 can regulate GFAP assembly via the Rho signalling pathway. Interestingly, all Trk family proteins can directly interact with an intermediate filament, peripherin (MacDonald *et al.*, 1999). All together, neurotrophins may be involved in regulation of cell morphology via cytoskeletal proteins such as intermediate filaments as well as microfilaments and microtubules (Etienne-Manneville & Hall, 2002).

Regulation of astrocytic morphology by BDNF–T1

In the adult mammalian CNS, BDNF is synthesized and secreted from pre- and postsynaptic neurons in a manner that depends on neuronal activity (Fawcett *et al.*, 1997, 1998; Aloyz *et al.*, 1999; Hartmann *et al.*, 2001; Kohara *et al.*, 2001). However, the physiological function of BDNF in the adult CNS remains unclear. One of the reasons that the function of BDNF in the adult mammalian CNS has not yet been clarified is that the function of T1, the major receptor for BDNF in the adult mammalian CNS from mice to nonhuman primates, has yet to be

addressed (Allendoerfer *et al.*, 1994; Fryer *et al.*, 1996; Ohira *et al.*, 1999). In the adult monkey prefrontal cortex, TK+/TK– heterodimers and TK–/TK– homodimers are formed in a BDNF-dependent manner; however, TK+/TK+ homodimers that function during development are not observed (Ohira *et al.*, 2001). These lines of evidence suggested that TK– (i.e. T1 in the adult neocortex) plays an important role in the maintenance and plasticity of the adult neocortex. Indeed, recent studies have demonstrated the function and signalling pathway of T1 (Rose *et al.*, 2003; Ohira *et al.*, 2005a; Ohira *et al.*, 2006). Thus, these studies provide clues to the elucidation of *in vivo* function of BDNF in the mature CNS.

T1 is expressed in both neurons and glial cells (Armanini *et al.*, 1995; Ohira *et al.*, 2005b), and it is highly involved in the regulation of the morphology of both types of cell (Yacoubian & Lo, 2000; Ohira *et al.*, 2005a). In terms of function, glial cells, and especially astrocytes, have been thought to play only a supportive role for neurons. However, recent studies have demonstrated that glial cells regulate the clearance of neurotransmitters, and that they maintain neural plasticity by themselves undergoing morphological changes (Theodosis & Poulain, 1993; Iino *et al.*, 2001; Oliet *et al.*, 2001; Theodosis *et al.*, 2004). In contrast, neuronal morphology in the adult rodent neocortex has been shown to be more static than previously thought (Grutzendler *et al.*, 2002). The findings of the present study are thus consistent with these previous findings. In the adult CNS, BDNF release might induce morphological changes in those astrocytic processes surrounding synapses via the T1 signalling pathway, eventually leading to rapid changes in synaptic strength and transmission (Wenzel *et al.*, 1991). However, it remains unclear whether or not the site-specific release of BDNF regulates astrocytic morphology and affects synaptic transmission and plasticity *in vivo* as well as in tissue slices.

It is reasonable to expect that BDNF treatment induces neurons to release factors that in turn regulate astrocytic morphology. In this study, we did not directly test this possibility. However, considering that (i) T1 regulates astrocytic morphology in astrocyte primary cultures in which the *in vivo* expression pattern of BDNF receptors is maintained (Ohira *et al.*, 2005a), and (ii) T1-specific siRNA electroporated into astrocytes suppressed BDNF-induced morphological changes in astrocytes, we concluded that the astrocytic morphology in the acute slices observed here was regulated by the BDNF–T1 signalling pathway in the astrocytes themselves.

In the present study, $GFAP^+$ astrocytic processes exhibited BDNF-dependent elongation of up to 15 μm, whereas previous studies have reported changes in process length of only several micrometers in the astrocytes of the brainstem (Hirrlinger *et al.*, 2004) and hippocampus (Benediktsson *et al.*, 2005). Previous reports have noted the spontaneous elongation and retraction of fine processes of protoplasmic astrocytes, in which glutamate, ATP and other factors would be expected to be involved in the regulation of astrocytic morphology (Volterra & Meldolesi, 2005). As *in vivo* BDNF release from synapses is regulated by neuronal activity, a bath application of BDNF would be expected to continuously stimulate astrocytes and result in a stronger elongation and branching effect among astrocytic processes. However, this effect may also reflect a difference between protoplasmic and fibrous astrocytes.

Functional significance of BDNF–T1 in neocortical layer I astrocytes

It is of note that, in the adult rat neocortex, the strongest BDNF immunoreactivity is observed in layer I (Yan *et al.*, 1997), which suggests that BDNF is enriched and functions in neocortical layer I. Neocortical layer I contains a small number of neurons and is composed predominantly of dendritic and axonal connections (Lund & Wu, 1997) which receive feedback inputs from the cortex (Rockland & Virga, 1989) and inputs from the thalamic nuclei (Glenn *et al.*, 1982; Lachica & Casagrande, 1992) as well as from other subcortical regions (Tigges & Tigges, 1985). The apical dendrites of pyramidal neurons in layers II–VI reach layer I (Lund & Wu, 1997). Thus, layer I is an important region in which the feedforward and feedback information from higher cortical areas, as well as from other lower cortical areas and subcortical regions, could be associated (Zhu & Zhu, 2004). Moreover, neocortical layer I is a network layer which would exert a direct and concerted effect on the firing properties of pyramidal cells in the deep layers (Chu *et al.*, 2003; Shlosberg *et al.*, 2003). In this context, one might consider whether or not the spillover of BDNF from a certain active synapse would affect the neighbouring inactive synapses. If so, the entanglement of neuronal wires would ensue, which would be quite detrimental to neuronal function. Therefore, in order to block the leakage of neurotransmitters and other functional molecules, as well as that of BDNF, from active synapses, the astrocytes that surround active synapses may alter their morphology in response to a spillover of BDNF; in this case, astrocytes could be considered an 'insulator' of synapses. At the same time, these morphological changes among astrocytes may regulate synaptic transmission in active synapses via the release of neurotransmitters from the astrocytes themselves; in this case, astrocytes would act as an 'amplifier' of transmission (Bezzi *et al.*, 2004; Fiacco & McCarthy, 2004).

Implications of T1 and morphological changes among astrocytes and neurons in terms of adult neural plasticity

According to the current paradigm, long-term morphological changes among neurons are fundamental to learning and memory. In the present model there exists a possible mechanism for the morphological alteration of neurons and astrocytes in which BDNF–T1 signalling may also be involved.

Long-term changes in glial processes in the living brain may exert an influence on neuronal morphology. For example, the adult hypothalamo-neurohypophysial system undergoes activity-dependent morphological plasticity which modifies astrocytic coverage of its oxytocinergic neurons and their synaptic inputs. Interestingly, reduced coverage of astrocytes at synaptic sites can be maintained for 1 month by lactation (Theodosis & Poulain, 1993; Theodosis *et al.*, 2004); this finding suggests that continuous neuronal stimulation can alter as well as maintain glial morphology. In addition, such glial changes can induce morphological changes in synapses (Theodosis & Poulain, 1993; Theodosis *et al.*, 2004). In other words, a prior morphological change in the glial cells might orientate neurons with respect to sites for dendrite elongation and synapse formation. Additional studies will be needed to further clarify the changes in neuronal fine structures.

Acknowledgements

We would like to thank Dr Hans Thoenen for his helpful suggestions and comments, Dr Keiji Wada for the gift of YFP transgenic mice, and Ms Tomoko Kohno, Ms Mikako Sakurai and Ms Hiromi Fujita for genotyping of YFP mice. This work was supported by grants from the Ministry of Education, Culture, Sports, Science and Technology of Japan [no. 18700343 to K.O., no. 15016056 to M.H., nos 16200025, 17022020 and 17650100 to T.K., no. 16015341 to S.N., the Biodiversity Research of 21st Century COE (A14)] and the Organization of Pharmaceutical Safety and Research (nano-1), a Sasakawa Scientific Research Grant from The Japan Science Society, and a Core Research for Evolutional Science and Technology (CREST) grant from the Japan Science and Technology Agency (JST).

Abbreviations

BDNF, brain-derived neurotrophic factor; GFAP, glial fibrillary acidic protein; GFP, green fluorescent protein; NGF, nerve growth factor; NT, neurotrophin; S-D, Sprague–Dawley; siRNA, small interfering RNA; TrkB, tropomyosin-related kinase B; TUNEL, terminal deoxynucleotidyl transferase-mediated digoxigenin nucleotide nick-end labelling; YFP, yellow fluorescent protein.

References

Allendoerfer, K.L., Cabelli, R.J., Escanòn, E., Kaplan, D.R., Nikolics, K. & Shatz, C.J. (1994) Regulation of neurotrophin receptors during the maturation of the mammalian visual system. *J. Neurosci.*, **14**, 1795–1811.

Aloyz, R., Fawcett, J.P., Kaplan, D.R., Murphy, R.A. & Miller, F.D. (1999) Activity-dependent activation of TrkB neurotrophin receptors in the adult CNS. *Learn. Mem.*, **6**, 216–231.

Araque, A., Parpura, V., Sanzgiri, R.P. & Haydon, P.G. (2001) Tripartite synapses: glia, the unacknowledged partner. *Trends Neurosci.*, **22**, 208–215.

Armanini, M.P., McMahon, S.B., Sutherland, J., Shelton, D.L. & Phillips, H.S. (1995) Truncated and catalytic isoforms of trkB are co-expressed in neurons of rat and mouse CNS. *Eur. J. Neurosci.*, **7**, 1403–1409.

Barbacid, M. (1994) The Trk family of neurotrophin receptors. *J. Neurobiol.*, **25**, 1386–1403.

Benediktsson, A.M., Schachtele, S.J., Green, S.H. & Dailey, M.E. (2005) Ballistic labeling and dynamic imaging of astrocytes in organotypic hippocampal slice cultures. *J. Neurosci. Meth.*, **141**, 41–53.

Bezzi, P., Gundersen, V., Galbete, J.L., Seifert, G., Steinhauser, C., Pilati, E. & Volterra, A. (2004) Astrocytes contain a vesicular compartment that is competent for regulated exocytosis of glutamate. *Nat. Neurosci.*, **7**, 613–620.

Bibel, M. & Barde, Y.A. (2000) Neurotrophins: key regulators of cell fate and cell shapes in the vertebrate nervous system. *Genes Dev.*, **14**, 2919–2937.

Bushong, E.A., Martone, M.E., Jones, Y.Z. & Ellisman, M.H. (2002) Protoplasmic astrocytes in CA1 striatum radiatum occupy separate anatomical domains. *J. Neurosci.*, **22**, 183–192.

Chu, Z., Galarreta, M. & Hestrin, S. (2003) Synaptic interactions of late-spiking neocortical neurons in layer 1. *J. Neurosci.*, **23**, 96–102.

Colombo, J.A., Fuchs, E., Härtig, W., Marotte, L.R. & Puissant, V. (2000) 'Rodent-like' and 'primate-like' types of astroglial architecture in the adult cerebral cortex of mammals: a comparative study. *Anat. Embryol.*, **201**, 111–120.

Etienne-Manneville, S. & Hall, A. (2002) Rho GTPases in cell biology. *Nature*, **420**, 629–635.

Fawcett, J.P., Aloyz, R., McLean, J.H., Pareek, S., Miller, F.D., McPherson, P.S. & Murphy, R.A. (1997) Detection of brain-derived neurotrophic factor in a vesicular fraction of brain synaptosomes. *J. Biol. Chem.*, **272**, 8837–8840.

Fawcett, J.P., Bamji, S.X., Causing, C.G., Aloyz, R., Ase, A.R., Reader, T.A., McLean, J.H. & Miller, F.D. (1998) Functional evidence that BDNF is an anterograde neuronal trophic factor in the CNS. *J. Neurosci.*, **18**, 2808–2821.

Fellin, T. & Carmignoto, G. (2004) Neurone-to-astrocyte signalling in the brain represents a distinct multifunctional unit. *J. Physiol. (Lond.)*, **559**, 3–15.

Feng, G., Mellor, R.H., Bernstein, M., Keller-Peck, C., Nguyen, Q.T., Wallace, M., Nerbonne, J.M., Lichtman, J.W. & Sanes, J.R. (2000) Imaging neuronal subsets in transgenic mice expressing multiple spectral variants of GFP. *Neuron*, **28**, 41–51.

Fiacco, T.A. & McCarthy, K.D. (2004) Intracellular astrocyte calcium waves in situ increase the frequency of spontaneous AMPA receptor currents in CA1 pyramidal neurons. *J. Neurosci.*, **24**, 722–732.

Fryer, R.H., Kaplan, D.R., Feinstein, S.C., Radeke, M.J., Grayson, D.R. & Kromer, L.F. (1996) Developmental and mature expression of full-length and truncated TrkB receptors in the rat forebrain. *J. Comp. Neurol.*, **374**, 21–40.

Glenn, L.L., Hada, J., Roy, J.P., Deschênes, M. & Steriade, M. (1982) Anterograde tracer and field potential analysis of the neocortical layer I projection from nucleus ventralis medialis of the thalamus in cat. *Neuroscience*, **7**, 1861–1877.

Grutzendler, J., Kasthuri, N. & Gan, W.B. (2002) Long-term dendritic spine stability in the adult cortex. *Nature*, **420**, 812–816.

Hartmann, M., Heumann, R. & Lessmann, V. (2001) Synaptic secretion of BDNF after high-frequency stimulation of glutamatergic synapses. *EMBO J.*, **20**, 5887–5897.

Hirrlinger, J., Hülsmann, S. & Kirchhoff, F. (2004) Astroglial processes show spontaneous motility at active synaptic terminals in situ. *Eur. J. Neurosci.*, **20**, 2235–2239.

Iino, M., Goto, K., Kakegawa, W., Okado, H., Sudo, M., Ishiuchi, S., Miwa, A., Takayasu, Y., Saito, I., Tsuzuki, K. & Ozawa, S. (2001) Glia–synapse interaction through Ca^{2+}-permeable AMPA receptors in Bergmann glia. *Science*, **292**, 926–929.

Kachi, S., Oshima, Y., Esumi, N., Kachi, M., Zack, D.J. & Campochiaro, P.A. (2005) Nonviral ocular gene transfer. *Gene Ther.*, **12**, 843–851.

Klein, R., Conway, D., Parada, L.F. & Barbacid, M. (1990) The trkB tyrosine kinase gene codes for a second neurogenic receptor that lacks the catalytic kinase domain. *Cell*, **61**, 647–656.

Kohara, K., Kitamura, A., Morishima, M. & Tsumoto, T. (2001) Activity-dependent transfer of brain-derived neurotrophic factor to postsynaptic neurons. *Science*, **291**, 2419–2423.

Kondoh, T., Motooka, Y., Bhattacharjee, A.K., Kokunai, T., Saito, N. & Tamaki, N. (2000) In vivo gene transfer into the periventricular region by electroporation. *Neurol. Med. Chir. (Tokyo)*, **40**, 618–623.

Kosako, H., Amano, M., Yanagida, M., Tanabe, K., Nishi, Y., Kaibuchi, K. & Inagaki, M. (1997) Phosphorylation of glial fibrillary acidic protein at the same sites by cleavage furrow kinase and Rho-associated kinase. *J. Biol. Chem.*, **272**, 10333–10336.

Lachica, E.A. & Casagrande, V.A. (1992) Direct W-like geniculate projections to the cytochrome oxidase (CO) blobs in primate visual cortex: axon morphology. *J. Comp. Neurol.*, **319**, 141–158.

Langle, S.L., Poulain, D.A. & Theodosis, D.T. (2003) Induction of rapid, activity-dependent neuronal-glial remodeling in the adult rat hypothalamus *in vitro*. *Eur. J. Neurosci.*, **18**, 206–214.

Lund, J.S. & Wu, C.Q. (1997) Local circuit neurons of macaque monkey striate cortex. IV. Neurons of laminae 1–3A. *J. Comp. Neurol.*, **384**, 109–126.

MacDonald, J.I.S., Verdi, J.M. & Meakin, S.O. (1999) Activity-dependent interaction of the intercellular domain of rat TrkA with intermediate filament proteins, the β-6 proteasomal subunit, Ras-GRF1, and the p162 subunit of eIF3. *J. Mol. Neurosci.*, **13**, 141–158.

Matsui, K., Jahr, C.E. & Rubio, M.E. (2005) High-concentration rapid transients of glutamate mediate neural-glial communication via ectopic release. *J. Neurosci.*, **25**, 7538–7547.

Middlemas, D.S., Lindberg, R.A. & Hunter, T. (1991) trkB, a neural receptor protein-tyrosine kinase: evidence for a full-length and two truncated receptors. *Mol. Cell. Biol.*, **11**, 143–153.

Miller, R.H. & Raff, M.C. (1984) Fibrous and protoplasmic astrocytes are Biochemically and developmentally distinct. *J. Neurosci.*, **4**, 585–592.

Ohira, K., Funatsu, N., Nakamura, S. & Hayashi, M. (2004) Expression of BDNF and TrkB receptor subtypes in the postnatal developing Purkinje cells of monkey cerebellum. *Gene Expr. Patterns*, **4**, 257–261.

Ohira, K. & Hayashi, M. (2003) Expression of TrkB subtypes in the adult monkey cerebellar cortex. *J. Chem. Neuroanat.*, **25**, 175–183.

Ohira, K., Homma, K.J., Hirai, H., Nakamura, S. & Hayashi, M. (2006) TrkB-T1 Regulates the RhoA signaling and actin cytoskeleton in glioma cells. *Biochem. Biophys. Res. Commun.*, **342**, 867–874.

Ohira, K., Kumanogoh, H., Sahara, Y., Homma, K.J., Hirai, H., Nakamura, S. & Hayashi, M. (2005a) A truncated tropo-myosine-related kinase B receptor, T1, regulates glial cell morphology via Rho GDP dissociation inhibitor 1. *J. Neurosci.*, **25**, 1343–1353.

Ohira, K., Shimizu, K. & Hayashi, M. (1999) Change of expression of full-length and truncated TrkBs in the developing monkey central nervous system. *Dev. Brain Res.*, **112**, 21–29.

Ohira, K., Shimizu, K. & Hayashi, M. (2001) TrkB dimerization during development of the prefrontal cortex of the macaque. *J. Neurosci. Res.*, **65**, 463–469.

Ohira, K., Shimizu, K., Yamashita, A. & Hayashi, M. (2005b) Differential expression of the truncated TrkB receptor, T1, in the primary motor and prefrontal cortices of the adult macaque monkey. *Neurosci. Lett.*, **385**, 105–109.

Okabe, S., Miwa, A. & Okado, H. (2001) Spine formation and correlated assembly of presynaptic and postsynaptic molecules. *J. Neurosci.*, **21**, 6105–6114.

Oliet, S.H., Piet, R. & Poulain, D.A. (2001) Control of glutamate clearance and synaptic efficacy by glial coverage of neurons. *Science*, **292**, 923–926.

Paxinos, G. & Watson, C. (1986) The rat brain in stereotaxic coordinates, 2nd Edn. Academic Press, San Diego.

Peters, A., Palay, S.L., de Webster, H. & F. (1976) *The Fine Structure of the Nervous System: the Neurons and Supporting Cells*. W.B. Saunders Co., Philadelphia, pp. 242–244.

Raff, M.C., Abney, E.R., Cohen, J., Lindsay, R. & Noble, M. (1983) Two types of astrocytes in cultures of developing rat white matter: differences in morphology, surface gangliosides, and growth characteristics. *J. Neurosci.*, **3**, 1289–1300.

Rockland, K.S. & Virga, A. (1989) Terminal arbors of individual 'feedback' axons projecting from area V2 to V1 in the macaque monkey: a study using

immunohistochemistry of anterogradely transported Phaseolus vulgaris-leucoagglutinin. *J. Comp. Neurol.*, **285**, 54–72.

Rose, C.R., Blum, R., Pichler, B., Lepier, A., Kafitz, K.W. & Konnerth, A. (2003) Truncated TrkB-T1 mediates neurotrophin-evoked calcium signalling in glia cells. *Nature*, **426**, 74–78.

Shlosberg, D., Patrick, S.L., Buskila, Y. & Amitai, Y. (2003) Inhibitory effect of mouse neocortex layer 1 on the underlying cellular network. *Eur. J. Neurosci.*, **18**, 2751–2759.

Theodosis, D.T., Piet, R., Poulain, D.A. & Oliet, S.H.R. (2004) Neuronal, glial and synaptic remodeling in the adult hypothalamus: functional consequences and role of cell surface and extracellular matrix adhesion molecules. *Neurochem. Int.*, **45**, 491–501.

Theodosis, D.T. & Poulain, D.A. (1993) Activity-dependent neuronal-glial and synaptic plasticity in the adult mammalian hypothalamus. *Neuroscience*, **57**, 501–535.

Tigges, J. & Tigges, M. (1985) Subcortical sources of direct projections to visual cortex. In Peters, A. & Jones, E.G. (eds), *Cerebral Cortex: Visual Cortex*, **Vol. 3**. Plenum Press, New York, pp. 351–378.

Ventura, R. & Harris, K.M. (1999) Three-dimensional relationships between hippocampal synapses and astrocytes. *J. Neurosci.*, **19**, 6897–6906.

Volterra, A. & Meldolesi, J. (2005) Astrocytes, from brain glue to communication elements: the revolution continues. *Nat. Rev. Neurosci.*, **6**, 626–640.

Wenzel, J., Lammert, G., Meyer, U. & Krug, M. (1991) The influence of long-term potentiation on the spatial relationship between astrocyte processes and potentiated synapses in the dentate gyrus neuropil of rat brain. *Brain Res.*, **560**, 122–131.

Wiesenhofer, B., Kaufmann, W.A. & Humpel, C. (1999) Improved lipid-mediated gene transfer in C6 glioma cells and primary glial cells using FuGene. *J. Neurosci. Meth.*, **92**, 145–152.

Yacoubian, T.A. & Lo, D.C. (2000) Truncated and full-length TrkB receptors regulate distinct modes of dendritic growth. *Nat. Neurosci.*, **3**, 342–349.

Yan, Q., Rosenfeld, R.D., Matheson, C.R., Hawkins, N., Lopez, O.T., Bennett, L. & Welcher, A.A. (1997) Expression of brain-derived neurotrophic factor protein in the adult rat central nervous system. *Neuroscience*, **78**, 431–448.

Zhu, Y. & Zhu, J.J. (2004) Rapid arrival and integration of ascending sensory information in layer 1 nonpyramidal neurons and tuft dendrites of layer 5 pyramidal neurons of the neocortex. *J. Neurosci.*, **24**, 1272–1279.

Available online at www.sciencedirect.com
ScienceDirect
Neurochemistry International 50 (2007) 119–129
NEUROCHEMISTRY International
www.elsevier.com/locate/neuint

Dopaminergic neuronal loss in transgenic mice expressing the Parkinson's disease-associated UCH-L1 I93M mutant

Rieko Setsuie [a,b,1], Yu-Lai Wang [a,1], Hideki Mochizuki [c,d], Hitoshi Osaka [a,e], Hideki Hayakawa [c], Nobutsune Ichihara [f], Hang Li [a], Akiko Furuta [a], Yae Sano [a,b], Ying-Jie Sun [a], Jungkee Kwon [a,g], Tomohiro Kabuta [a], Kenji Yoshimi [d], Shunsuke Aoki [a], Yoshikuni Mizuno [c,d], Mami Noda [b], Keiji Wada [a,*]

[a] *Department of Degenerative Neurological Diseases, National Institute of Neuroscience, National Center of Neurology and Psychiatory, Kodaira, Tokyo 187-8502, Japan*
[b] *Laboratory of Pathophysiology, Graduate School of Pharmaceutical Sciences, Kyushu University, Higashi-ku, Fukuoka 812-8582, Japan*
[c] *Department of Neurology, Juntendo University School of Medicine, Bunkyo-ku, Tokyo 113-8421, Japan*
[d] *Research Institute for Diseases of Old Age, Juntendo University School of Medicine, Bunkyo-ku, Tokyo 113-8421, Japan*
[e] *Division of Neurology, Clinical Research Institute, Kanagawa Children's Medical Center, Yokohama 232-8555, Japan*
[f] *Department of Anatomy, School of Veterinary Medicine, Azabu University, Sagamihara 229-8501, Japan*
[g] *College of Veterinary Medicine, Chonbuk National University, 644-14 Duckjin-Ku, Jeonju 561-756, Republic of Korea*

Received 14 March 2006; received in revised form 19 June 2006; accepted 11 July 2006
Available online 11 September 2006

Abstract

The I93M mutation in ubiquitin carboxyl-terminal hydrolase L1 (UCH-L1) was reported in one German family with autosomal dominant Parkinson's disease (PD). The causative role of the mutation has, however, been questioned. We generated transgenic (Tg) mice carrying human *UCHL1* under control of the *PDGF-B* promoter; two independent lines were generated with the I93M mutation (a high- and low-expressing line) and one line with wild-type human UCH-L1. We found a significant reduction in the dopaminergic neurons in the substantia nigra and the dopamine content in the striatum in the high-expressing I93M Tg mice as compared with non-Tg mice at 20 weeks of age. Although these changes were absent in the low-expressing I93M Tg mice, 1-methyl-4-phenyl-1,2,3,6-tetrahydropyridine (MPTP) treatment profoundly reduced dopaminergic neurons in this line as compared with wild-type Tg or non-Tg mice. Abnormal neuropathologies were also observed, such as silver staining-positive argyrophilic grains in the perikarya of degenerating dopaminergic neurons, in I93M Tg mice. The midbrains of I93M Tg mice contained increased amounts of insoluble UCH-L1 as compared with those of non-Tg mice, perhaps resulting in a toxic gain of function. Collectively, our data represent *in vivo* evidence that expression of *UCHL1*^{I93M} leads to the degeneration of dopaminergic neurons.

Keywords: Ubiquitin carboxy-terminal hydrolase L1; Animal model; Parkinson's disease; Dopaminergic neuron

1. Introduction

Parkinson's disease (PD) is the second most common human neurodegenerative disorder after Alzheimer's disease (AD) (Dauer and Przedborski, 2003; Vila and Przedborski, 2004). PD patients exhibit motor dysfunction, including slowed movement (bradykinesia), resting tremor, rigidity, and postural instability (Dauer and Przedborski, 2003). The pathological basis of PD is the progressive loss of dopaminergic neurons in the substantia nigra pars compacta, giving rise to a decrease in dopamine content in the striatum (Dauer and Przedborski, 2003). Although most cases of PD are sporadic, studies of familial PD have provided accumulating evidence for the molecular mechanisms of PD. Thus far, at least six proteins have been identified to cause familial PD: α-synuclein (Chartier-Harlin et al., 2004; Farrer et al., 2004; Ibanez et al., 2004; Kruger et al., 1998; Polymeropoulos et al., 1997; Singleton et al., 2003), UCH-L1 (Leroy et al., 1998), parkin (Kitada et al., 1998), DJ-1 (Bonifati et al., 2003), phosphatase

* Corresponding author. Tel.: +81 42 346 1715; fax: +81 42 346 1745.
E-mail address: wada@ncnp.go.jp (K. Wada).
[1] These authors contributed equally to this work.

0197-0186/$ – see front matter © 2006 Elsevier Ltd. All rights reserved.
doi:10.1016/j.neuint.2006.07.015